Low temperature nitriding of AISI 300 and 200 series austenitic stainless steels

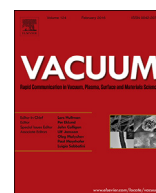(Article begins on next page)

Dear Author,

Please, note that changes made to the HTML content will be added to the article before publication, but are not reflected in this PDF.

Note also that this file should not be used for submitting corrections.

Low temperature nitriding of AISI 300 and 200 series austenitic stainless steels

Francesca Borgioli[*], Emanuele Galvanetto, Tiberio Bacci

Department of Industrial Engineering (DIEF), University of Florence, via S. Marta 3, 50139 Florence, Italy

ABSTRACT

In this study the effects of low temperature plasma nitriding on the characteristics of different austenitic stainless steels, CrNi-based (AISI 304L and AISI 316L) and CrMn-based (AISI 202), were compared. Samples were nitrided at 400 and 430 °C, at 1000 Pa for 5 h, and their microstructure, phase composition, microhardness and corrosion resistance were evaluated. The characteristics of modified surface layers depended on both treatment parameters and alloy composition. For all the steels modified surface layers had a double layer microstructure. In the outer modified layer, mainly consisting of S phase, deformation (or shear) bands were observed in the grains, and nitrogen induced h.c.p. martensite, ε'_N, formed. The tendency to form shear bands and ε'_N was higher for AISI 202 samples, and decreased for AISI 304L and then for AISI 316L ones, influencing the modified layer thickness. When nitriding was performed at 430 °C, nitrides formed, and their amount was affected by steel composition. Nitriding treatments allowed to markedly increase surface microhardness and corrosion resistance, in comparison with the untreated alloys. When nitrides did not form, as for the 400-°C nitrided samples, the corrosion behaviour of the considered steels was comparable. Nitride precipitation affected corrosion resistance, increasing corrosion phenomena.

© 2016 Published by Elsevier Ltd.

1. Introduction

Austenitic stainless steels are employed in many industrial fields thanks to their corrosion resistance, ease of formability and weldability. Their very good corrosion resistance in many aggressive environments is due to the presence of a surface passive film, mainly consisting of chromium oxide, which is self healing if damaged and protects the alloy from the surrounding medium [1]. The face centred cubic structure of these alloys is maintained owing to the presence of austenite stabilizing elements, like nickel, manganese and nitrogen. Fairly high amounts of nickel (usually 8 wt% or higher) are present in the so called AISI 300 series stainless steels, which are widely used. Nickel is partly substituted by manganese and nitrogen in the cheaper AISI 200 series stainless steels, which have higher strength; however, these alloys may show lower corrosion resistance than AISI 300 series steels, due to the lower chromium content [2].

The industrial applications of austenitic stainless steels may be limited by their low hardness and poor tribological properties, which may compromise the performance of components subjected to wear. Moreover, in spite of the very good resistance to general corrosion, these alloys suffer localised corrosion in specific environments, especially in chloride-ion containing solutions. Among the surface engineering techniques, employed to improve wear and corrosion resistance properties of austenitic stainless steels, low temperature nitriding has received increasing attention in the last years [1,3]. Treatment temperatures lower than 450 °C allow to avoid the precipitation of large amounts of chromium nitrides and the consequent decrease of corrosion resistance [4]. In this manner, a supersaturated solid solution of nitrogen in the expanded and distorted austenite lattice is produced, known as S phase [1,3,4] or expanded austenite [1,3,5], which has high hardness and improved corrosion resistance in chloride-ion containing solutions [3,4]. Many researches were devoted to study the structure [3,4,6–11] and the properties [3–5,12–15] of this phase, and the treatment techniques able to produce it [3,5,16–18]. These studies were usually carried out using a single steel type, in order to put in evidence the effects of different nitriding techniques [3,16–18] or treatment parameters [3,13,14,18–20]. The effect of steel composition was investigated especially regarding the influence of nickel

* Corresponding author.
  E-mail address: francesca.borgioli@unifi.it (F. Borgioli).

2　　　　　　　　　　　　　　　　　　F. Borgioli et al. / Vacuum xxx (2016) 1–10

[3,21−23], molybdenum [24−26], and chromium [3,21,23,27]. Recent studies also regarded steels with low amounts of alloy elements like copper and niobium [26], or the high nitrogen and nickel-free stainless steels with improved biocompatibility [28,29]. The analysis of the scientific literature shows that the used steels are mainly of the 300 series [3,5,6,25,26]; limited studies regarded low-nickel alloys, as 17Cr−15Mn−4N [30] and X50CrNiNbN 21 9 [31], or the nickel-free F2581 [29], which have a niche use. The direct comparison of the effects of nitriding on AISI 300 and 200 stainless steels has received little attention. Even if a comparison could be performed using the results obtained by different researches, it is hindered by the fact that different experimental conditions, and, in particular, nitriding parameters, were usually used.

In the present research a direct comparison of the effects of low temperature nitriding on the characteristics of the modified surface layers produced on AISI 300 and 200 series austenitic stainless steels was performed. Three steels of large commercial use were chosen, CrNi grades AISI 304L and AISI 316L, and the low-nickel CrMn grade AISI 202. Glow-discharge nitriding technique was used to perform nitriding treatments. The microstructure, phase composition, hardness and corrosion resistance characteristics of the nitrided samples were investigated and they were compared with those of the untreated alloys.

2. Experimental procedure

Three austenitic stainless steels were used, AISI 202, AISI 304L and AISI 316L, supplied by ThyssenKrupp Acciai Speciali Terni (Italy); the chemical composition of the steels is reported in Table 1. The steels, in the form of cold rolled, annealed and pickled plates, were cut in order to obtain prismatic samples (40 × 17 × 0.7 mm). The surface finishing of the samples was classified as 2D according to the EN 10088-2:2005 norm [32]. The surfaces, which had to be treated, were not ground and polished further; their average surface roughness, Ra, was 0.16 ± 0.02 μm, and their maximum height of profile, Rz, was 1.8 ± 0.1 μm. As an example, the surface morphology of an untreated AISI 202 sample is shown in Fig. 1.

Low temperature glow-discharge nitriding treatments were carried out in a laboratory plasma equipment, previously described [33]. The treatment parameters were chosen on the basis of our previous results [13]. Before the treatments, the treatment chamber was evacuated up to a pressure of about 5 Pa; the required treatment pressure was maintained by a flow controlled dynamic vacuum system. Before the nitriding step, cathodic sputtering was performed in order to remove the natural passive film and enable a homogeneous nitriding process, operating at 130 Pa with 80 vol% N_2 and 20 vol% H_2 up to 310 °C. After this step, the temperature and pressure were increased up to their nominal values. Nitriding treatments were carried out at 400 or 430 °C, at a constant pressure of 1000 Pa, for 5 h, using a gas mixture of 80 vol% N_2 and 20 vol% H_2 in a 300 sccm total flow rate. The current density values depended on the treatment temperature, and they were 2.5 ± 0.1 mA cm^{-2} for the 400-°C treatment, and 2.8 ± 0.1 mA cm^{-2} for the 430-°C treatment; the voltage drop was 190 ± 10 V.
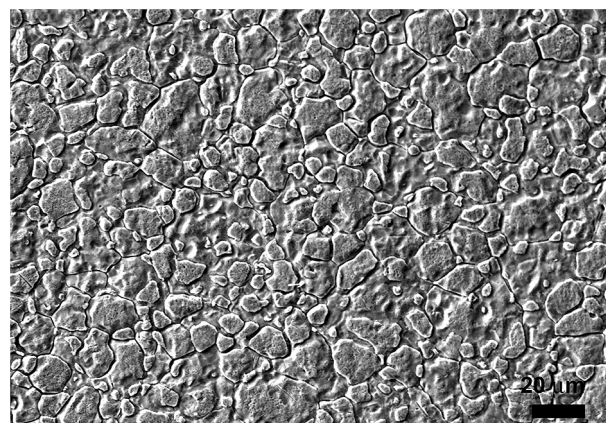

Fig. 1. Surface morphology of an untreated AISI 202 sample.

The microstructure of the nitrided and untreated samples was examined using light and scanning electron microscopies and energy dispersion spectroscopy (EDS) analysis. EDS analysis, performed on unetched samples using a 20 kV accelerating voltage for the electron beam, allowed to obtain a semi-quantitative evaluation of the amount of the alloy elements (Fe, Cr, Ni, Mo, Mn, Si) and of nitrogen in different zones of the samples. In order to observe the cross-section microstructure of the modified layers, samples were cut and mounted using glass-filled epoxy thermosetting resin. Tapered sections with a 1.5°-angle were obtained for selected samples by cold mounting them in epoxy resin. The microstructure of the modified surface layers and of the matrix was delineated by means of glyceregia etchant.

The phases present in the surface layers were identified by means of X-ray diffraction analysis (Cu Kα radiation). Diffraction patterns were collected in Bragg-Brentano configuration and with constant incident angles in the range 10−35°; in this latter configuration, the mean penetration depth (i.e. the depth at which the intensity drops by a factor of e) ranges from 0.6 μm ($\alpha = 10°$) to 1.47 μm ($\alpha = 35°$).

Roughness measurements were performed on the surface of the samples before and after the treatments by using a stylus profilometer tester (cut-off length: 0.8 mm). At least five measurements were taken at different locations on the surface. The average surface roughness Ra (arithmetical mean deviation of the roughness profile from the mean line) and the maximum height of profile Rz (sum of the largest profile peak height and the largest profile valley depth within a sampling length, according to EN ISO 4287-2009 norm) were recorded.

Surface microhardness measurements (load: 50 gf) and depth profiles (load: 10 gf) were performed on the samples using a Knoop indenter.

Corrosion resistance of untreated and nitrided samples was studied in aerated 5% NaCl solution at room temperature. A three-electrode electrochemical flat cell equipped with Ag/AgCl reference electrode (3.5 M KCl) and a platinum grid as counterelectrode was used. The sample surface area exposed to the electrolyte was 1 cm^2. Polarization measurements were performed potentiodynamically at a sweep rate of 0.3 mV s^{-1} after a delay period of 22 h. Three corrosion tests for each sample type were carried out for assessing the result.

Table 1
Chemical composition (wt.%) of the used austenitic stainless steels.

Material	Composition							
	C	Si	Mn	Cr	Ni	Mo	N	Fe
AISI 202	0.065	0.40	7.7	17.0	4.1	−	0.15	Bal.
AISI 304L	0.028	0.30	1.7	18.0	8.0	0.27	0.065	Bal.
AISI 316L	0.029	0.34	0.9	16.6	10.3	2.01	0.049	Bal.

3. Results

3.1. Morphology and microstructure

The untreated samples have an austenitic microstructure. X-ray diffraction analysis shows that, beyond austenite, γ-Fe (f.c.c.), small peaks of α-Fe (b.c.c.) are present in the steels.

The nitriding treatments produce modified surface layers, the characteristics of which depend on the treatment temperature and the used alloy; the thickness of the modified layers is reported in Table 2.

When the steels were nitrided at 400 °C, the modified surface layers have a double layer microstructure, as shown in Fig. 2. The single layers, delineated by chemical etching, are homogeneous and they are separated one from the other and from the matrix by etched lines. Thicker modified layers are present on AISI 202 samples in comparison with those on AISI 304L and AISI 316L, as observed by both microscopy analysis and nitrogen concentration depth profiles (Fig. 3). In the outer layer of all the sample types, groups of thin lines, which extend from the outer surface into the layer itself, are observed. In the AISI 202 samples many lines are present, and they extend deeply in the layer (Fig. 2a). In the AISI 304L steel the lines are slightly fewer and they extend less deeply (Fig. 2b). Even fewer and less deep lines are observed in the AISI 316L alloy (Fig. 2c). The presence of these lines, usually related to the local plastic deformations occurring during the formation of the modified layers, was previously reported [3,5,6,12,13]. This microstructure can be better observed in the tapered sections of the samples. As shown in Fig. 4, many parallel and intersecting lines are present in the grains near the outer surface. This microstructure is comparable with that of a plastically deformed austenitic stainless steel, in which deformation bands, also referred to as shear bands, are present [34—36]. Shear band has been defined as a collective term for planar defects that form during plastic deformation as a result of the overlapping of stacking faults on austenite {111} planes [1,34].

X-ray diffraction analysis, performed with a 10°-incident angle, suggests that the outer modified layer mainly consists of S-phase (Fig. 5). The peaks of a solid solution of nitrogen in h.c.p. martensite, ε'_N, are also present. The amount of this phase is the greatest in AISI 202 samples (Fig. 5a), and it decreases in the AISI 300 series samples, with the smallest amount in the AISI 316L steel (Fig. 5c). This nitrogen induced martensite is considered analogous to the strain induced h.c.p. martensite [37], but with larger lattice parameters due to nitrogen solubilisation, and it differs from ε-type h.c.p. $M_{2\text{-}3}N$ (M = Fe, Mn, Cr, Mo, Ni) nitride, which has an ordered nitrogen arrangement.

For all the sample types the inner modified layer is fairly homogenous and it does not show the presence of deformation bands. X-ray diffraction analysis, performed increasing the incident angle up to 35°, suggests that this layer consists of a solid solution of interstitial atoms (nitrogen, carbon) in the slightly expanded austenite lattice, γ(N,C) (Fig. 6).

When the samples were nitrided at 430 °C, the modified surface layers still show the characteristic double layer microstructure (Fig. 7). The thickness of the outer modified layer is the greatest for AISI 316L samples, and it decreases for AISI 304L and then for AISI 202 ones, which have the smallest thickness, as observed by both microscopy analysis and nitrogen concentration depth profiles (Fig. 8). Many strongly etched regions, which correspond to nitrides, are observed in the cross-sections of the outer modified layer of AISI 202 and AISI 304L samples, being present inside the grains, along the shear lines and along the parent austenite grain boundaries. On AISI 316L these regions are fewer and they are observed only along the grain boundaries. As also observed previously [13,33], in the zones corresponding to these etched regions, an increase of chromium, manganese and molybdenum content, and a decrease of nickel content are detected by EDS analysis, in comparison with the values detected in the zones corresponding to the S phase, the γ(N,C) phase and the matrix, which have a comparable composition. As an example, for AISI 202 in these regions chromium increases up to 26.8 wt% and manganese up to 10.2 wt%, while nickel decreases up to 3.2 wt%; for AISI 316L chromium increases up to 26.3 wt%, manganese up to 2.4 wt% and molybdenum up to 4.4 wt%, while nickel decreases up to 7.1 wt%. This result is in accordance with the fact that chromium, manganese and molybdenum are strong nitride forming elements, while nickel is not.

X-ray diffraction analysis, performed both in Bragg-Brentano configuration and using a 15°-constant incident angle, suggests that, at this nitriding temperature, chromium nitride, CrN (f.c.c.), is also able to form (Figs. 9 and 10). In fact, the main peaks of this nitride, at about 37.5° and 43.5°, fully overlap the peaks of ε'_N martensite, but a distinctive peak of this phase is observable at about 63.5° as a fairly broad shoulder of the S-phase peak, allowing its identification (Fig. 10). The presence of ε-type $M_{2\text{-}3}N$ nitride, which may form as a consequence of a distortion of the h.c.p. structure of ε'_N martensite and of an ordering of nitrogen atoms [38], is supposed on the basis of microscopy analysis, even if distinct peaks are not observed.

The average surface roughness, Ra, of all the sample types tends to increase as the nitriding temperature increases, ranging from 0.18 ± 0.02 (400 °C) to 0.23 ± 0.02 (430 °C) μm; a similar trend was observed for the maximum height of profile, Rz, which ranges from 2.2 ± 0.1 (400 °C) to 2.5 ± 0.1 (430 °C) μm.

3.2. Microhardness

Surface microhardness values of untreated and nitrided samples are shown in Fig. 11.

The surface microhardness of the nitrided samples is greater than that of the untreated ones for all the considered steels, and it tends to increase as the treatment temperature is increased. When nitriding was performed at 400 °C, AISI 202 samples have the greatest microhardness values, also in accordance with the greatest thickness of the modified layers for this steel type. When the samples were nitrided at 430 °C, the presence of hard and brittle nitrides influences the behaviour of the samples, with the highest values measured for AISI 304L samples.

The microhardness profiles of the nitrided samples are shown in Fig. 12. In the modified layers of all the sample types the detected hardness values are high, and they decrease to matrix value in a fairly steep way. The obtained results are in good agreement with morphology observations and nitrogen concentration depth profiles: when the thickness of the modified layers is greater, a thicker hardened layer is observed. Moreover, higher hardness values are detected when the treatment temperature is higher, as observed for surface microhardness measurements.
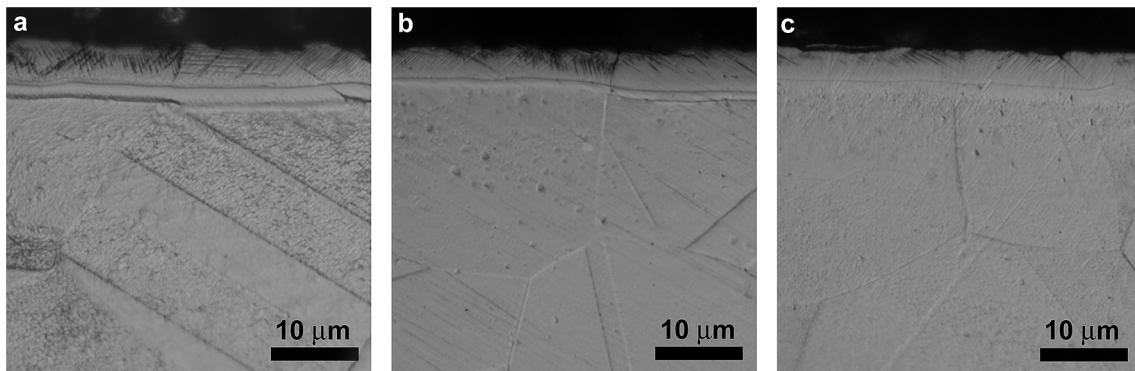
Table 2
Thickness of the outer (d_o) and inner (d_i) modified layers of austenitic stainless steel samples nitrided at different temperatures (T).

Steel type	T (°C)	d_o (μm)	d_i (μm)
AISI 202	400	4.7 ± 0.6	2.0 ± 0.3
AISI 304L	400	4.4 ± 0.4	1.3 ± 0.2
AISI 316L	400	4.3 ± 0.4	1.4 ± 0.1
AISI 202	430	7.3 ± 0.8	2.2 ± 0.3
AISI 304L	430	9.0 ± 0.5	2.5 ± 0.3
AISI 316L	430	9.9 ± 0.6	2.5 ± 0.4

Fig. 2. Micrographs of the modified surface layers of AISI 202 (a), AISI 304L (b) and AISI 316L (c) austenitic stainless steel samples nitrided at 400 °C (cross-section; etchant: glyceregia).
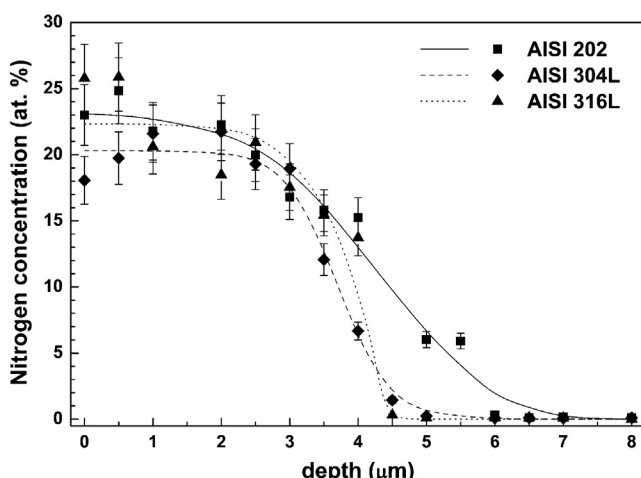

Fig. 3. Nitrogen concentration depth profiles of AISI 202, AISI 304L and AISI 316L austenitic stainless steel samples nitrided at 400 °C (the lines are drawn as a guide for the eye).
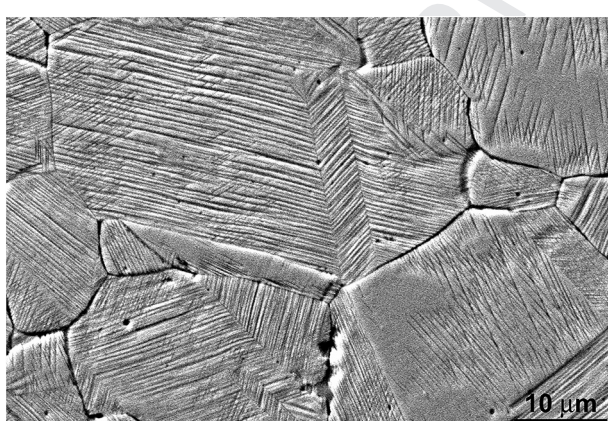

Fig. 4. SEM micrograph of a detail of the outer modified layer of an AISI 202 austenitic stainless steel sample nitrided at 400 °C (1.5°-tapered section; the marker refers to the length in the tapered section) (etchant: glyceregia).

3.3. Corrosion behaviour

Polarization curves of untreated and nitrided samples, tested in 5% NaCl aerated solution, are shown in Fig. 13. The average
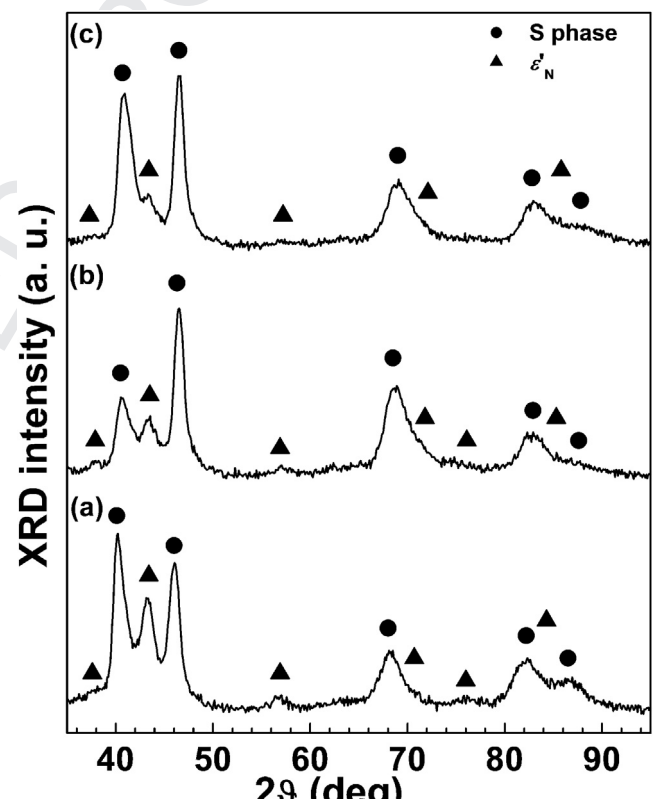

Fig. 5. X-ray diffraction patterns of AISI 202 (a), AISI 304L (b) and AISI 316L (c) austenitic stainless steel samples nitrided at 400 °C (configuration: 10°-incident angle).

corrosion potential, passive current density and pitting potential (evaluated as the potential beyond which the anodic current density last crossed 5 μA cm^{-2} before the end of the corrosion tests) are reported in Table 3.

The polarization curves of all the sample types are typical of passive materials subjected to localised corrosion when the potential value is higher than a threshold.

For the untreated samples of all the tested steels, low anodic current values are detected in the passive branch, and they show a fast increase when localised corrosion occurs. At the highest potential values, anodic current density values are limited by concentration polarization phenomena. As expected, the lowest corrosion potential values are observed for AISI 202 samples (about
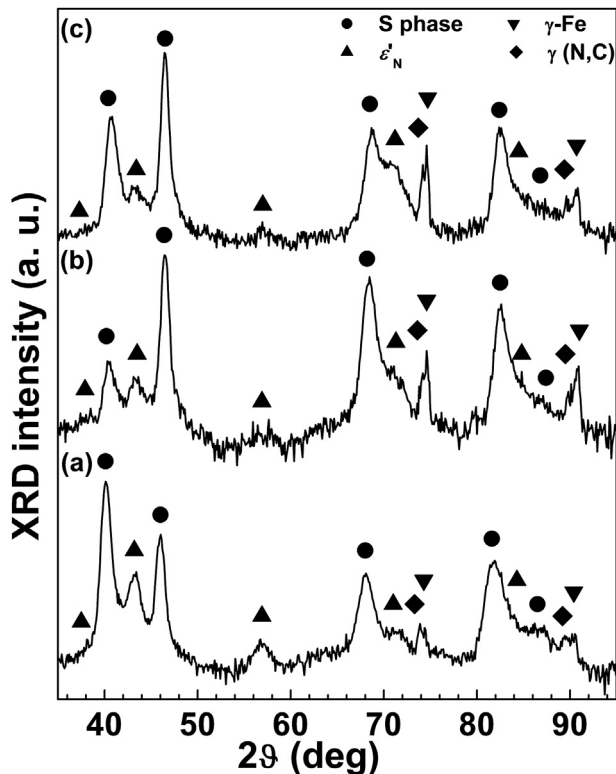
Fig. 6. X-ray diffraction patterns of AISI 202 (a), AISI 304L (b) and AISI 316L (c) austenitic stainless steel samples nitrided at 400 °C (configuration: 35°-incident angle).
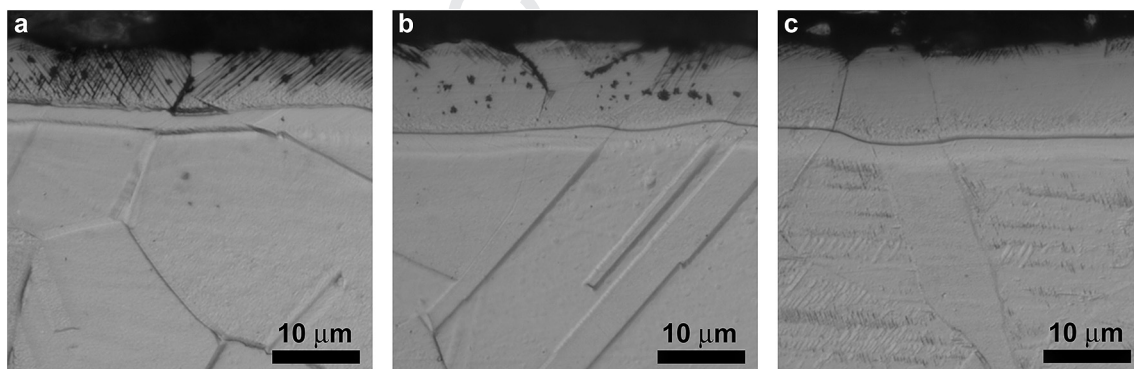

Fig. 8. Nitrogen concentration depth profiles of AISI 202, AISI 304L and AISI 316L austenitic stainless steel samples nitrided at 430 °C (the lines are drawn as a guide for the eye).

samples.

When nitriding was performed at 400 °C, after the tests, the surface of all the sample types is fairly untouched, and it shows only few coloured regions, in correspondence of which very shallow pits are observed (Fig. 14 d–f).

For the samples nitrided at 430 °C, the potential values, at which localised corrosion occurs, tend to decrease, in comparison with the values detected for the samples nitrided at 400 °C. After the tests, the surface of the samples is lightly coloured and many shallow pits

Fig. 7. Micrographs of the modified surface layers of AISI 202 (a), AISI 304L (b) and AISI 316L (c) austenitic stainless steel samples nitrided at 430 °C (cross-section; etchant: glyceregia).

- 144 mV (Ag/AgCl)) (Fig. 13a), while the highest ones are observed for AISI 316L samples (about - 92 mV (Ag/AgCl)) (Fig. 13c). A similar trend is registered when the potential value, at which localised corrosion phenomena begin, is considered. After the tests, the surface of the samples shows many large and deep pits, randomly distributed on the surface (Fig. 14 a–c). The pits have a vertical development, due to the vertical position of the samples during the corrosion tests. Moreover, crevice corrosion occurred in the area shielded by the PTFE gasket. The damage due to corrosion is the highest on AISI 202 samples (Fig. 14a), while it is the lowest on AISI 316L samples (Fig. 14c), in accordance with the polarization data.

For all the nitrided samples significantly nobler corrosion potential values are observed, and localised corrosion begins at potentials which are markedly higher than those of untreated
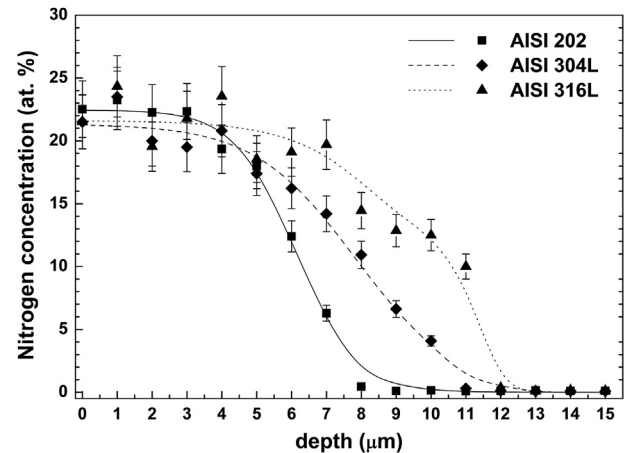
are present (Fig. 14 g–i). The number of pits is greater on AISI 202 samples (Fig. 14 g), while it tends to decrease on AISI 316L ones (Fig. 14 i).

4. Discussion

Low temperature nitriding is recognised as an effective surface engineering technique for improving surface hardness and corrosion resistance of austenitic stainless steels. It is a general agreement that this improvement is due to the formation of the supersaturated solid solution of nitrogen in the expanded and distorted austenite lattice, named S phase, and that the treatment temperature should not exceed about 450 °C in order to avoid the precipitation of large amounts of chromium nitrides. However, the
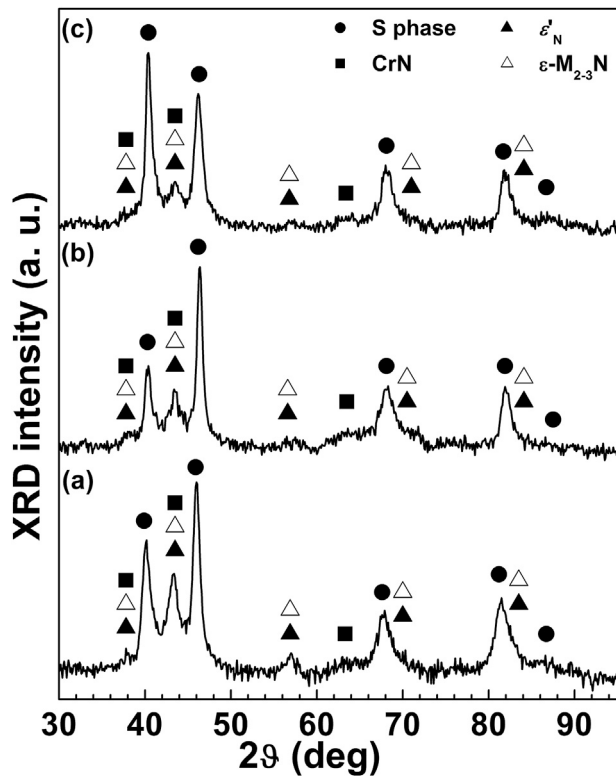
Fig. 9. X-ray diffraction patterns of AISI 202 (a), AISI 304L (b) and AISI 316L (c) austenitic stainless steel samples nitrided at 430 °C (configuration: Bragg-Brentano).
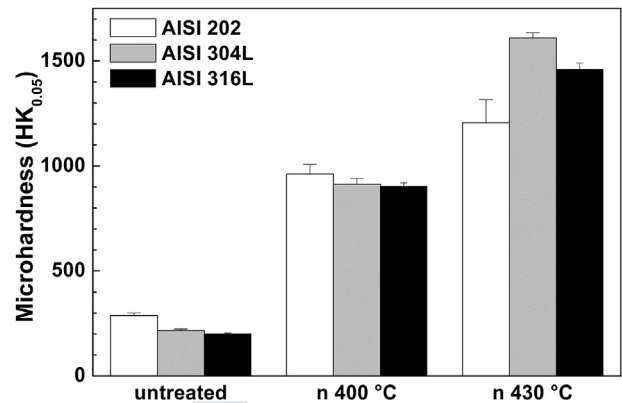

Fig. 10. X-ray diffraction patterns of AISI 202 (a, d), AISI 304L (b, e) and AISI 316L (c, f) austenitic stainless steel samples nitrided at 430 °C. The details (d, e, f) were obtained increasing the scan time-per-step (configuration: 15°-incident angle).

Fig. 11. Surface Knoop microhardness values of AISI 202, AISI 304L and AISI 316L samples untreated and nitrided as indicated.
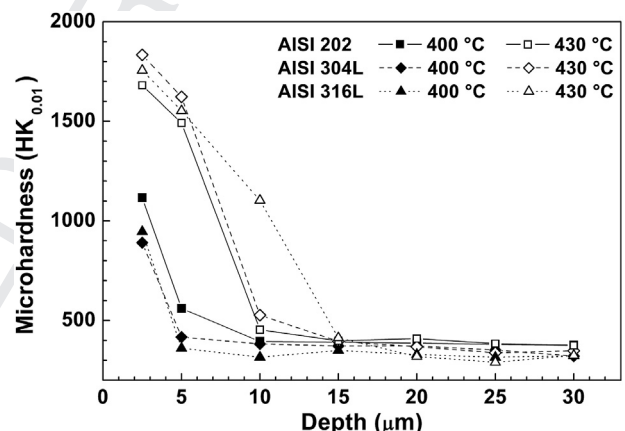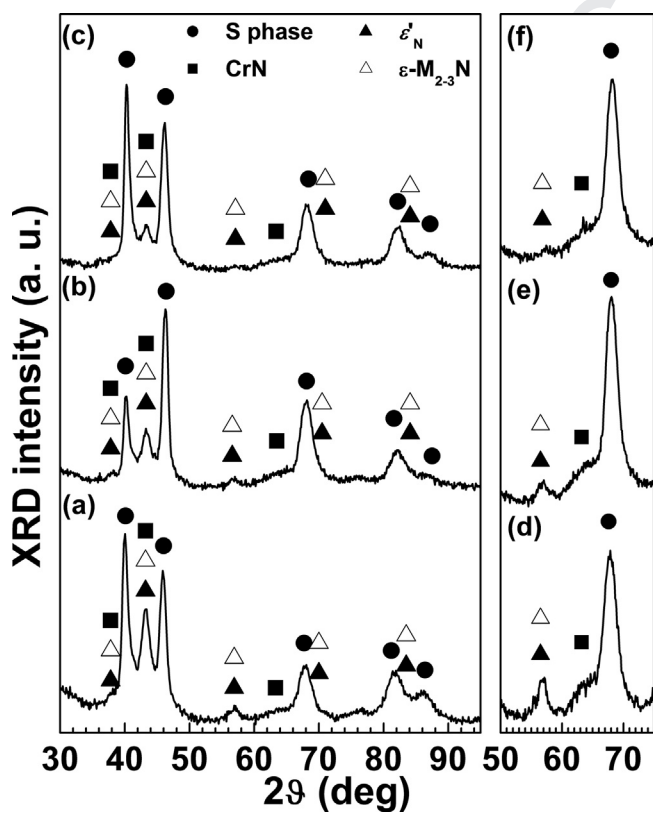

Fig. 12. Knoop microhardness profiles of AISI 202, AISI 304L and AISI 316L samples untreated and nitrided as indicated.

analysis of the scientific literature suggests that both nitriding conditions and alloy composition play important roles in influencing the characteristics of the modified surface layers.

In this research a direct comparison of the effects of low temperature glow-discharge nitriding, performed at two different temperatures (400 and 430 °C) on three different steels, was performed. AISI 304L and AISI 316L, which are largely employed, were chosen as representative of the 300 series stainless steels. These steels, in their higher carbon counterparts, AISI 304 and AISI 316, were considered for comparison in other researches [6,22,26]. On the other hand, 200 series stainless steels are usually neglected as possible candidate for nitriding, and few studies are present [33,39]. These steels may be attractive for their higher strength and lower cost, so AISI 202 was chosen as their representative.

When nitriding was performed, all the considered steels are able to form modified surface layers with a double layer microstructure. This microstructure, previously observed on AISI 202 [33,39], was explicitly reported also for some 300-series stainless steels by a few authors [5,17,22,39–43], but it is also observable in the micrographs present in other researches [3,6,12,15,20,26,29]. X-ray diffraction analysis suggests that this double layer structure is formed by a thicker outer layer, in which an expanded austenite with larger lattice parameter, i.e. S phase, is present, and by a thinner inner layer, consisting of an expanded austenite with smaller lattice parameter. This latter phase, indicated as $\gamma(N, C)$ in the present research, was hypothesised either to be due to an accumulation of
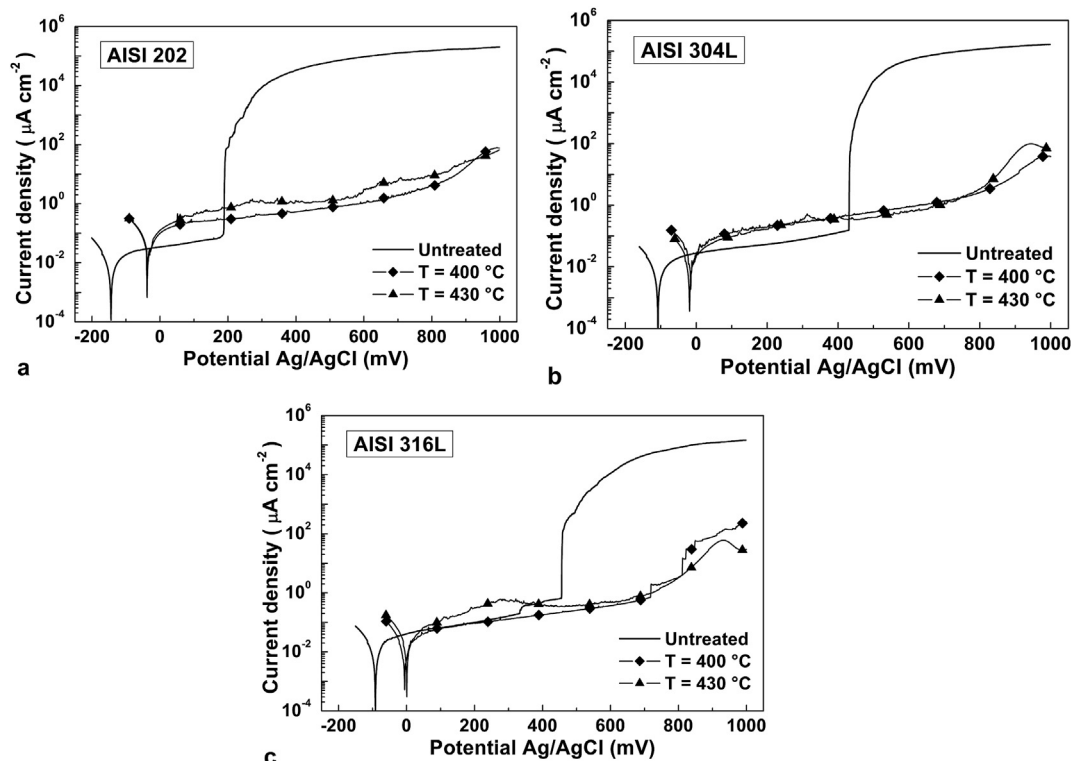
Fig. 13. Polarization curves of AISI 202 (a), AISI 304L (b) and AISI 316L (c) austenitic stainless steel samples untreated and nitrided as indicated (solution: 5% NaCl, aerated).

Table 3

Average corrosion potential, E_{corr}, passive current, i_p, and pitting potential, E_{pit}, of AISI 202, AISI 304L and AISI 316L samples untreated or nitrided as indicated (solution: 5% NaCl, aerated). The pitting potential was evaluated as the potential beyond which the anodic current density last crossed 5 μA cm^{-2} before the end of the corrosion tests.

Sample type	E_{corr} (mV (Ag/AgCl))	i_p (μA cm^{-2})	E_{pit} (mV (Ag/AgCl))
AISI 202 — untreated	−144 ± 20	0.04 ± 0.01	+190 ± 30
AISI 202 — nitr. 400 °C	−37 ± 20	0.60 ± 0.08	+824 ± 30
AISI 202 — nitr. 430 °C	−38 ± 20	0.9 ± 0.1	+685 ± 30
AISI 304L — untreated	−108 ± 20	0.06 ± 0.01	+432 ± 30
AISI 304L — nitr. 400 °C	−16 ± 20	0.48 ± 0.08	+835 ± 30
AISI 304L — nitr. 430 °C	−19 ± 20	0.52 ± 0.08	+780 ± 30
AISI 316L — untreated	−92 ± 20	0.09 ± 0.02	+457 ± 30
AISI 316L — nitr. 400 °C	−5 ± 20	0.20 ± 0.08	+811 ± 30
AISI 316L — nitr. 430 °C	+1 ± 20	0.42 ± 0.08	+803 ± 30

carbon atoms at the end of nitrogen profile [40—42], or to be related to the high residual stresses induced between the expanded austenite layer and the substrate [22], or to be due to the presence of nitrogen atoms which are not trapped by chromium [43]. Analysis of nitrogen and carbon depth profiles, performed on AISI 202 samples, did not show conclusive evidence of a carbon rich inner layer [33]. Even if the presence of carbon atoms in γ(N, C) may be hypothesised on the basis of the alloy composition, the fact that comparable thickness of this inner layer is observed for steels having both high (AISI 202) and low (AISI 304L and 316L) carbon contents suggests that carbon accumulation is not the main cause of the formation of this layer and that the production of S phase plays a key role.

In the modified surface layers, nitride formation is influenced not only by nitriding conditions, but also by steel composition. Nitriding temperature has usually been considered the main parameter to control when a nitride-free modified layer is desired.

However, even if low temperatures are used, nitride precipitation is not always avoided. By using a nitriding temperature of 400 °C, a nitride-free layer was obtained on AISI 304, AISI 316 and their lower carbon counterparts by many authors [6,11,14,20—22,26], in accordance with the results obtained in the present research. The additional presence of chromium nitrides was observed when plasma ion implantation or beam ion implantation were employed [16], or when the treatment time of plasma nitriding was increased, even with durations shorter [31] or comparable [12] with respect to those used by us. On the other hand, nitrides were not detected on AISI 316LVM samples plasma nitrided at 430 °C [29], or on gas treated AISI 316L [5] and pulsed plasma treated AISI 304 [14] using a nitriding temperature as high as 450 °C, while they were present on AISI 304 and AISI 316 plasma nitrided at 430 °C [26]. Regarding AISI 202 steel, nitrides were not formed when it was nitrided at 400 °C and 1000 Pa, as shown previously [33] and in the present research, while they formed when the treatment pressure was decreased at 500 Pa [39]. Thus, the nitride precipitation is influenced by nitriding techniques together with all the treatment parameters controlling the nitrogen amount which can be absorbed by steel surface. However, the use of different nitriding temperatures may be suitable for studying the tendency of different steels to form or not nitrides.

The results obtained in the present research suggest that AISI 202 has the highest tendency to form nitrides, as expected for a steel having a great content of manganese, which is a nitride forming element, and a small content of nickel, which is not able to form nitrides. When 300 series stainless steels are considered, AISI 304L shows a higher tendency to form nitrides than AISI 316L. This fact, observed also by Egawa et al. [26], was ascribed to the tendency of molybdenum atoms to stabilise the structure of S phase by attracting nitrogen atoms around themselves, so that the precipitation of chromium nitrides is prevented. It may also be hypothesised that ε'_N, which forms in large amounts in AISI 304L steel, acts
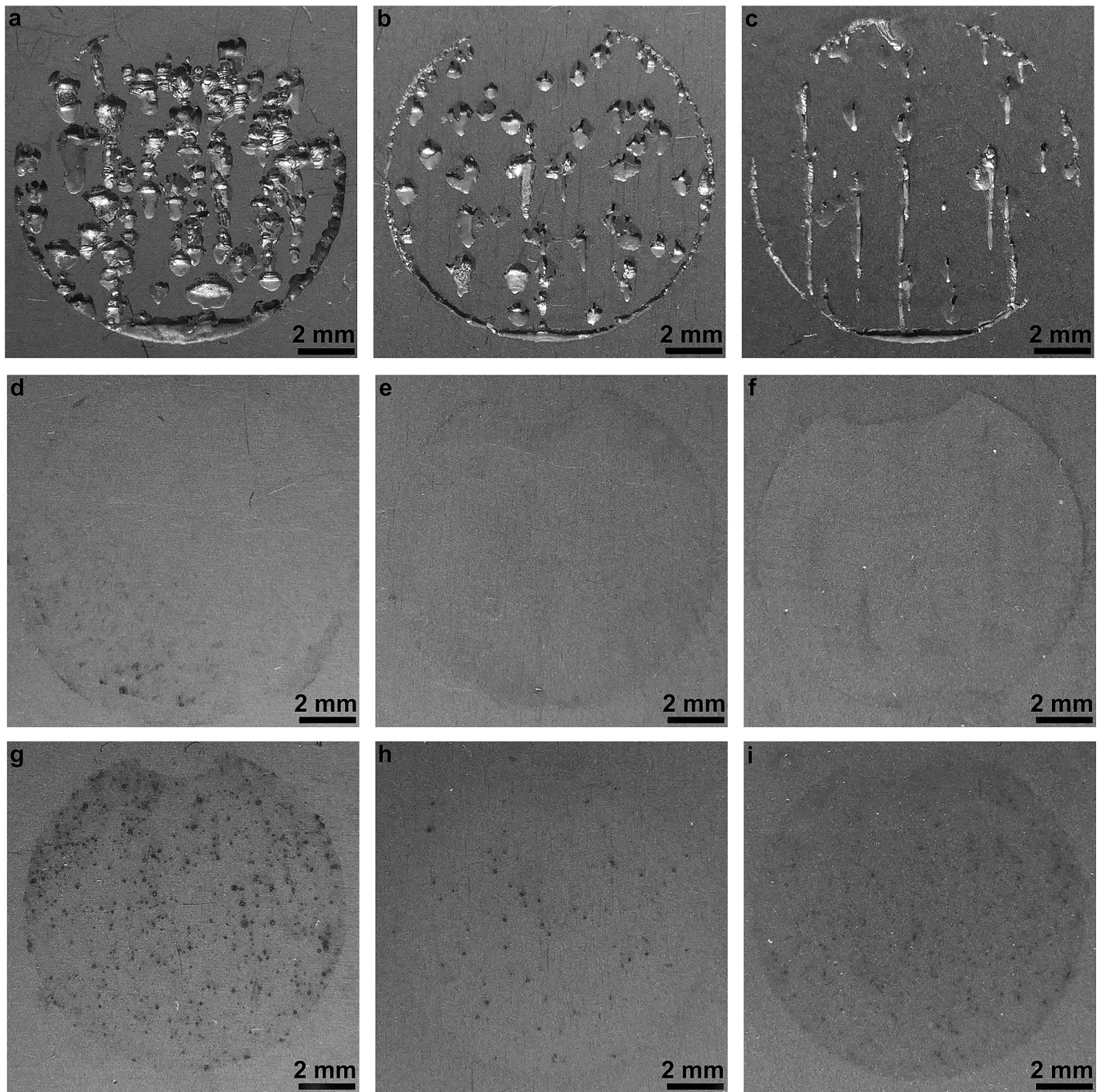
Fig. 14. Surface morphology after corrosion tests. Untreated samples: AISI 202 (a), AISI 304L (b), AISI 316L (c). 400-°C nitrided samples: AISI 202 (d), AISI 304L (e), AISI 316L (f). 430-°C nitrided samples: AISI 202 (g), AISI 304L (h), AISI 316L (i). (Solution: 5% NaCl, aerated).

as a precursor of h.c.p. ε-type nitride, as also suggested by Lei et al. [44]. It has to be noted that AISI 304L samples, nitrided at 430 °C, show the presence of a significantly greater amount of nitrides than that obtained by Egawa et al. [26] for samples plasma treated at the same temperature, especially in the intergranular regions.

The outer modified layer of all the samples shows the presence of shear bands and ε'_N martensite. While shear bands are usually observed in this layer [3,5,6,12,13], the presence of ε'_N was reported by few authors [5,33,37,39,45]. The formation of shear bands and ε'_N martensite is related to the formation of modified surface layers and to the alloy composition. The solubilisation of nitrogen atoms

in the austenite well beyond the solubility limit is able not only to expand and distort the f.c.c. lattice, but also to cause local plastic deformations, as previously reported [3,13]. When plastic deformation occurs in an austenitic stainless steel, a perfect dislocation may dissociate into two Shockley partial dislocations and form wide stacking faults, in which the ABCABC stacking, characteristic of a f.c.c. metal, becomes an ABAB stacking, characteristic of a h.c.p. structure [34,46]. When the intrinsic stacking faults overlap regularly on every second {111} plane, a plate of h.c.p. ε' martensite is formed. B.c.t. α' martensite may also nucleate at the intersection of ε' martensite laths [34,46]. It has been hypothesised that, when the

width of stacking faults diverges, shear bands extend through the austenite grains [34]. The formation of shear bands and ε' martensite is supposed to be favoured when the stacking fault energy (SFE) of the steel is low [34]. SFE depends on the chemical composition of the steels, so empirical relations have been proposed for its calculation [1]. Dai et al. [47] have suggested that the effects of alloy elements on SFE are not monotonous and interactions exist among these elements. According to their relation, the SFE at room temperature, γ^{300}, can be written as:

$$\gamma^{300} \, (\text{mJ/m}^2) = \gamma^0 + 1.59\text{Ni} - 1.34\,\text{Mn} + 0.06\,\text{Mn}^2 - 1.75\text{Cr}$$
$$+ 0.01\text{Cr}^2 + 15.21\text{Mo} - 5.59\text{Si} - 60.69(\text{C} + 1.2\text{N})^{1/2}$$
$$+ 26.27(\text{C} + 1.2\text{N})\,(\text{Cr} + \text{Mn} + \text{Mo})^{1/2} + 0.61[\text{Ni}\,(\text{Cr} + \text{Mn})]^{1/2}$$

where the elements are expressed in weight percentage and γ^0 is the SFE of pure γ-Fe at room temperature, which is supposed to be in the range $36 \div 42$ mJ m^{-2}. This relation can be used to evaluate the SFE of the steels used in the present research. According to the authors [47], the maximum value for (C + N) is 0.45, well below the nitrogen content in nitrided austenitic stainless steels (up to about 10 wt% [3]). So it was decided to neglect the N contribution in the calculus, and 'reduced' SFE values were obtained, that can be used for comparing the steels when they solubilise comparable nitrogen contents. It results that for AISI 202 'reduced' SFE ranges approx. $1 \div 7$ mJ m^{-2}, for AISI 304L $16 \div 22$ mJ m^{-2} and for AISI 316L $51 \div 57$ mJ m^{-2}. Even if the nitrogen solubilisation, due to the nitriding process, may decrease further on the SFE of all these alloys [48], it is expected that the tendency to form shear bands and ε' martensite increases from AISI 316L to AISI 304L and then to AISI 202, as indeed observed. It is interesting to note that, for samples nitrided at 400 °C, the thickness of the modified layers tends to increase in the same way, so that it may be supposed that shear bands act as fast diffusion paths for nitrogen atoms. As a consequence, slightly thicker and harder modified surface layers are produced on AISI 202 steel, in comparison with AISI 304L and AISI 316L alloys. The thickness of the modified layers of the 300-series stainless steels, about 5.7 μm as a whole, is comparable with that measured by Egawa et al. [26] for AISI 304 and AISI 316 samples plasma nitrided at 400 °C for 4 h, while it is significantly greater than that measured by Sun et al. [6] for samples of the same alloys nitrided at 400 °C for 5 h, but with a lower nitrogen content in the treatment atmosphere. When nitrides are able to precipitate, as in the 430-°C nitrided samples, the comparison of the thickness of the modified layers for the different steels suggests that the formation and the presence of nitrides are able to decrease the overall nitrogen diffusion rate, so that the thickest layers are observed when the lowest nitride content is present, i.e. on AISI 316L steel. The thickness values for AISI 304L and AISI 316L samples are slightly higher than those obtained by Egawa et al. [26] for AISI 304 and AISI 316 nitrided at the same temperature.

The presence of nitrides influences the surface hardness of the samples. Surface microhardness values, typical of a nitrogen rich S phase [3], are detected when the nitride amount is small, as for AISI 316L samples. The great amount of nitrides causes a marked hardness increase in AISI 304L samples. The lower hardness value and its fairly high standard deviation for AISI 202 samples suggest that the peculiar microstructure with a high content of ε'_N martensite and nitrides of this steel type causes an increase in brittleness.

The formation of modified layers consisting mainly of S phase, as those produced with 400-°C nitriding, allows to significantly increase the corrosion resistance of all the considered alloys. While steel composition markedly influences the occurrence of localised corrosion phenomena for the untreated samples, when S phase forms, the differences among the tested steels become much less

marked and a comparable corrosion behaviour is observed, in accordance with our previous results [39].

On the other hand, localised corrosion phenomena are observable on all the sample types nitrided at 430 °C, and they are related to the presence of nitride precipitates, which prevent the matrix to form a uniform and protective passive layer. As expected, the number of pits is the greatest on AISI 202 samples, which have the greatest amount of nitrides, while it is the smallest on AISI 316L samples, which have the smallest amount. However, it is interesting to note that, with the used treatment conditions, the corrosion phenomena are limited for all the studied steels, and corrosion resistance remains markedly higher than that of the untreated alloys.

5. Conclusions

Low temperature glow-discharge nitriding, carried out at 400 and 430 °C, at 1000 Pa for 5 h on AISI 202, AISI 304L and AISI 316L austenitic stainless steel samples produces modified surface layers, the characteristics of which depend on both the treatment parameters and alloy composition.

The modified surface layers of all the sample types have a double layer microstructure, with an outer layer, mainly consisting of S phase, and an inner layer, in which a solid solution of interstitial atoms in the slightly expanded austenite lattice, $\gamma(N,C)$, is present. In the outer modified layer the presence of shear bands and nitrogen induced h.c.p. martensite, ε'_N, is related to the stacking fault energy of the alloys, and it influences the thickness of the modified layers.

When nitriding was carried out at 400 °C, nitrides are not detected in the modified layers. The corrosion resistance of all these samples is significantly higher than that of the untreated ones, and the influence of alloy composition is much less marked, so that all the studied steels show a comparable corrosion behaviour.

When nitriding was performed at 430 °C, in the outer modified layers CrN and h.c.p. nitrides, ε-M$_{2-3}$N, form. Nitride formation is promoted by the decrease of nickel content and increase of manganese in the steel composition, so that nitride amount is greater on AISI 202 samples. The presence of nitrides causes a decrease in the corrosion resistance, which is more marked when greater amounts of nitrides precipitate, as on AISI 202 samples.

References

[1] K.H. Lo, C.H. Shek, J.K.L. Lai, Recent developments in stainless steels, Mater. Sci. Eng. R. 65 (2009) 39–104.

[2] J. Charles, The new 200 Series: an alternative answer to Ni surcharge? Dream or nightmare?, in: J.A. Odriozola, A. Paúl (Eds.), Stainless Steel '05, Proceedings of the Fifth Stainless Steel Science and Market Congress, Sevilla (Spain), September 27–30, 2005, Centro de Investigaciones Científicas Isla de la Cartuja, Sevilla, 2005, pp. 19–27.

[3] H. Dong, S-phase surface engineering of Fe-Cr-Co-Cr and Ni-Cr alloys, Int. Mater. Rev. 55 (2010) 65–98.

[4] T. Bell, Surface engineering of austenitic stainless steel, Surf. Eng. 18 (2002) 415–422.

[5] T. Christiansen, M.A.J. Somers, Low temperature gaseous nitriding and carburising of stainless steel, Surf. Eng. 21 (2005) 445–455.

[6] Y. Sun, X.Y. Li, T. Bell, X-ray diffraction characterisation of low temperature plasma nitrided austenitic stainless steels, J. Mater. Sci. 34 (1999) 4793–4802.

[7] S. Mändl, B. Rauschenbach, Anistotropic strain in nitrided austenitic stainless steel, J. Appl. Phys. 88 (2000) 3323–3328.

F. Borgioli et al. / Vacuum xxx (2016) 1–10

[8] T. Christiansen, M.A.J. Somers, On the crystallographic structure of S-phase, Scr. Mater. 50 (2004) 35–37.

[9] F. Borgioli, A. Fossati, E. Galvanetto, T. Bacci, G. Pradelli, Glow-discharge nitriding of AISI 316L austenitic stainless steel: Influence of treatment pressure, Surf. Coat. Technol. 200 (2006) 5505–5513.

[10] M.P. Fewell, J.M. Priest, High-order diffractometry of expanded austenite using synchrotron radiation, Surf. Coat. Technol. 202 (2008) 1802–1815.

[11] C. Templier, J.C. Stinville, P. Villechaise, P.O. Renault, G. Abrasonis, J.P. Rivière, A. Martinavičius, M. Drouet, On lattice plane rotation and crystallographic structure of the expanded austenite in plasma nitrided AISI 316L steel, Surf. Coat. Technol. 204 (2010) 2551–2558.

[12] L. Nosei, S. Farina, M. Ávalos, L. Náchez, B.J. Gómez, J. Feugeas, Corrosion behavior of ion nitrided AISI 316L stainless steel, Thin Solid Films 516 (2008) 1044–1050.

[13] A. Fossati, E. Galvanetto, T. Bacci, F. Borgioli, Improvement of corrosion resistance of austenitic stainless steels by means of glow-discharge nitriding, Corros. Rev. 29 (2011) 209–221.

[14] K. Köster, P. Kaestner, G. Bräuer, H. Hoche, T. Troßmann, M. Oechsner, Material condition tailored to plasma nitriding process for ensuring corrosion and wear resistance of austenitic stainless steel, Surf. Coat. Technol. 228 (2013) S615–S618.

[15] I. Flis-Kabulska, Y. Sun, J. Flis, Monitoring the near-surface pH to probe the role of nitrogen in corrosion behaviour of low-temperature plasma nitrided 316L stainless steel, Electrochim. Acta 104 (2013) 208–215.

[16] R. Wei, J.J. Vajo, J.N. Matossian, P.J. Wilbur, J.A. Davis, D.L. Williamson, G.A. Collins, A comparative study of bean ion implantation, plasma ion implantation and nitriding of AISI 304 stainless steel, Surf. Coat. Technol. 83 (1996) 235–242.

[17] T. Czerwiec, N. Renevier, H. Michel, Low-temperature plasma assisted nitriding, Surf. Coat. Technol. 131 (2000) 267–277.

[18] S.C. Gallo, H. Dong, Study of active screen plasma processing conditions for carburising and nitriding austenitic stainless steel, Surf. Coat. Technol. 203 (2009) 3669–3675.

[19] R.R.M. de Sousa, F.O. de Araújo, L.C. Gontijo, J.A.P. da Costa, C. Alves Jr., Cathodic cage plasma nitriding (CCPN) of austenitic stainless steel (AISI 316): influence of the different ratios of the (N_2/H_2) on the nitrided layers properties, Vacuum 86 (2012) 2048–2053.

[20] S. Wang, W. Cai, J. Li, W. Wei, J. Hu, A novel rapid D.C. plasma nitriding at low gas pressure for 304 austenitic stainless steel, Mater. Lett. 105 (2013) 47–49.

[21] E. Menthe, K.-T. Rie, J.W. Schultze, S. Simson, Structure and properties of plasma-nitrided stainless steels, Surf. Coat. Technol. 74–75 (1995) 412–416.

[22] D.L. Williamson, J.A. Davis, P.J. Wilbur, Effect of austenitic stainless steel composition on low-energy, high-flux, nitrogen ion beam processing, Surf. Coat. Technol. 103–104 (1998) 178–184.

[23] F. Pedraza, C. Savall, G. Abrasonis, J.P. Rivière, J.F. Dinhut, J.L. Grosseau-Poussard, Low energy, high-flux nitridation of face-centred cubic metallic matrices, Thin Solid Films 515 (2007) 3661–3669.

[24] S. Mändl, R. Günzel, E. Richter, W. Möller, B. Rauschenbach, Annealing behaviour of nitrogen implanted stainless steel, Surf. Coat. Technol. 128–129 (2000) 423–428.

[25] P. Saravanan, V.S. Raja, S. Mukherjee, Effect of alloyed molybdenum on corrosion behavior of plasma immersion nitrogen ion implanted austenitic stainless steel, Corr. Sci. 74 (2013) 106–115.

[26] M. Egawa, N. Ueda, K. Nakata, M. Tsujikawa, M. Tanaka, Effect of additive alloying element on plasma nitriding and carburizing behavior for austenitic stainless steels, Surf. Coat. Technol. 205 (2010) S246–S251.

[27] K. Gemma, T. Ohtsuka, T. Fujiwara, M. Kawakami, A new perspective for rapid nitriding in high Cr austenitic steels, J. Mater. Sci. 36 (2001) 5231–5235.

[28] J. Buhagiar, H. Dong, T. Bell, Low temperature plasma surface alloying of medical grade austenitic stainless steel with carbon and nitrogen, Surf. Eng.

[29] J. Buhagiar, X. Li, H. Dong, Formation and microstructural characterisation of S-phase layers in Ni-free austenitic stainless steels by low-temperature plasma surface alloying, Surf. Coat. Technol. 204 (2009) 330–335.

[30] K. Gemma, Y. Satoh, I. Ushioku, M. Kawakami, Abnormal nitriding behaviour of a high chromium, high manganese austenitic steel, Surf. Eng. 11 (1995) 240–245.

[31] J. Feugeas, B. Gómez, A. Craievich, Ion nitriding of stainless steels. Real time surface characterization by synchrotron X-ray diffraction, Surf. Coat. Technol. 154 (2002) 167–175.

[32] EN 10088-2:2005, Stainless Steels. Part 2: Technical Delivery Conditions for Sheet/plate and Strip of Corrosion Resisting Steels for General Purposes, European Committee for Standardization (CEN), Brussels, 2005.

[33] F. Borgioli, A. Fossati, G. Matassini, E. Galvanetto, T. Bacci, Low temperature glow-discharge nitriding of a low nickel austenitic stainless steel, Surf. Coat. Technol. 204 (2010) 3410–3417.

[34] J. Talonen, H. Hänninen, Formation of shear bands and strain-induced martensite during plastic deformation of metastable austenitic stainless steels, Acta Mater. 55 (2007) 6108–6118.

[35] A.K. De, D.C. Murdock, M.C. Mataya, J.G. Speer, D.K. Matlock, Quantitative measurement of deformation-induced martensite in 304 stainless steel by X-ray diffraction, Scr. Mater. 50 (2004) 1445–1449.

[36] S.M.M. Tavares, J.M. Pardal, M.J. Gomes da Silva, H.F.G. Abreu, M.R. da Silva, Deformation induced martensitic transformation in a 201 modified austenitic stainless steel, Mater. Charact. 60 (2009) 907–911.

[37] M.K. Lei, Phase transformations in plasma source ion nitrided austenitic stainless steel at low temperature, J. Mater. Sci. 34 (1999) 5975–5982.

[38] H. Jacobs, D. Rechenbach, U. Zachwieja, Structure determination of γ'-Fe_4N and ε-Fe_3N, J. Alloys Compd. 227 (1995) 10–17.

[39] F. Borgioli, A. Fossati, L. Raugei, E. Galvanetto, T. Bacci, Low temperature glow-discharge nitriding of stainless steels, in: Proceedings of the 7th European Stainless Steel Conference - Science and Market, Como (Italy), September 21–23, 2011, Associazione Italiana di Metallurgia, Milan, 2011 (CD-rom; ISBN: 978-88-85298-84-2).

[40] S. Mändl, B. Rauschenbach, Concentration dependent nitrogen diffusion coefficient in expanded austenite formed by ion implantation, J. Appl. Phys. 91 (2002) 9737–9742.

[41] T. Czerwiec, H. He, S. Weber, C. Dong, H. Michel, On the occurrence of dual diffusion layers during plasma-assisted nitriding of austenitic stainless steel, Surf. Coat. Technol. 200 (2006) 5289–5295.

[42] T. Michler, Influence of plasma nitriding on hydrogen environment embrittlement of 1.4301 austenitic stainless steel, Surf. Coat. Technol. 202 (2008) 1688–1695.

[43] T. Christiansen, K.V. Dahl, M.A.J. Somers, Nitrogen diffusion and nitrogen depth profiles in expanded austenite: experimental assessment, numerical simulation and role of stress, Mater. Sci. Tech. 24 (2008) 159–167.

[44] M.K. Lei, Y. Huang, Z.L. Zhang, In situ transformation of nitrogen-induced h.c.p. martensite in plasma source ion-nitrided austenitic stainless steel, J. Mater. Sci. Lett. 17 (1998) 1165–1167.

[45] W. Liang, X. Xiaolei, X. Jiujun, S. Yaqin, Characteristics of low pressure plasma arc source ion nitrided layer on austenitic stainless steel at low temperature, Thin Solid Films 391 (2001) 11–16.

[46] L. Bracke, G. Mertens, J. Penning, B.C. De Cooman, M. Liebeherr, N. Akdut, Influence of phase transformations on the mechanical properties of high-strength austenitic Fe-Mn-Cr steel, Metal. Mater. Trans. A 37A (2006) 307–317.

[47] Q.-X. Dai, A.-D. Wang, X.-N. Cheng, X.-M. Luo, Stacking fault energy of cryogenic austenitic steels, Chin. Phys. 11 (2002) 596–600.

[48] I.A. Yakubtsov, A. Ariapour, D.D. Perovic, Effect of nitrogen on stacking fault energy of f.c.c. iron-based alloys, Acta Mater. 47 (1999) 1271–1279.